Waveform Diversity: Past, Present, and Future

A. De Maio (IEEE Senior), A. Farina (IEEE Fellow, IET Fellow)

Abstract

Waveform diversity indicates the ability to adapt and diversify dynamically the waveform to the operating environment in order to achieve a performance gain over non-adaptive systems. This technique can allow one or more sensors to automatically change operating parameters such as frequency, pulse repetition time, transmit pattern, modulation, etc. The present lecture starts with an overview concerning the role of the waveform diversity in history, mathematics, and music from the epoch of Pythagoras, continuing with the studies of Galileo, Fourier, and Maxwell. Examples of waveform diversity in nature, such as the bat sonar signal, the sounds of whales, and the cosmic microwave background radiation are presented[1]. A tutorial introduction to the concept of ambiguity function, its relevant properties, and its role as an instrument to quantify the quality of a waveform, follows. Precisely, after a short review of the most common radar signals and their ambiguity functions, the effects of a possible signal coding is thoroughly described. Amplitude, phase, and frequency codes are considered, even if a special attention is deserved to the class of frequency coded waveforms through a Costas sequence.

Keywords. Ambiguity Function, Radar Coding, Waveform Diversity.

I. INTRODUCTION

The waveform exploited by the radar is responsible of resolution, accuracy, and ambiguity of the target range and radial velocity measurements. While range is associated with the delay of the received signal, radial velocity depends on the Doppler frequency shift.

Waveform design algorithms usually anticipated their implementation by many years, due to complexity and hardware limitations [1]. For instance, the concept of pulse compression,

Antonio De Maio is with Università degli Studi di Napoli “Federico II”, Dipartimento di Ingegneria Elettronica e delle Telecomunicazioni, Via Claudio 21, I-80125, Napoli, Italy. E-mail: ademaio@unina.it

Alfonso Farina is with SELEX - Sistemi Integrati, Via Tiburtina Km. 12.4, I-00131, Roma, Italy. E-mail: afarina@selex-si.com

[1]This first part is only the object of the oral presentation and is not explicitly reported in these notes.

developed during the World War II, gained renewed interest only when high-power Klystrons became available [2]. In other words, what seems unpractical today, may not be definitely ruled out in the near future. The lack of signal coherence, which precluded the application of signal compression during the World War II is today easy. Maybe, the linear power amplifiers, required to implement amplitude modulated radar signals, will not represent a technological limitation tomorrow.

If a matched filter is used at the receiver, the ambiguity function represents a suitable tool to study the response of the filter in two dimensions: delay and Doppler. The constant volume underneath the squared ambiguity function involves some trade-offs in signal design. Precisely, a narrow response in one dimension is accompanied by a poor response in the other dimension or by additional ambiguous peaks. Moreover, if we prefer ambiguous peaks to be well spaced in delay, we have to accept them closely spaced in Doppler (and vice versa). If we want a good Doppler resolution, we need long coherent signal durations.

Several signals are used for different radar applications and systems. Modern pulsed radars generally use pulse compression waveforms characterized by high pulse energy (with no increase in peak power) and large pulse bandwidth. As a consequence, they provide high range resolution without sacrificing maximum range which depends on the pulse energy.

Unfortunately, there are not easily-handled mathematical techniques to calculate a signal with a prescribed ambiguity function. It follows that the design of a radar signal with desirable characteristics of the ambiguity function is mainly based on the designer's prior knowledge of radar signatures as well as on "trial and check procedures".

In this lecture, we first present (Section II) the mathematical definition of the ambiguity function and describe its relevant properties[2]. Then, we will explore, in Section III, the ambiguity function of some basic radar signals: unmodulated rectangular pulse, Linear Frequency Modulated (LFM) pulse, and coherent pulse train. Hence, in Section IV, the conflicts in designing suitable waveforms for different applications are discussed: radar coding is presented as a suitable mean to achieve ambiguity function shaping. Several techniques based on frequency and phase coding are presented; the ultimate goal is to segregate the volume of the ambiguity function in regions of the delay-Doppler plane where it ceases to be a practical embarrassment [3]. In

[2]Some material in these notes is taken from [1].

Section V, the merits and the drawbacks concerning the use of coherent trains of diverse pulses is addressed. Finally concluding remarks are drawn in Section VI.

II. Ambiguity Function: Definition and Properties

This function was introduced in signal analysis by Ville [4] and in the radar context by Woodward [3]. However, it was known in thermodynamic, since 1932, due to Eugene Wigner (Nobel prize) who studied quantum corrections to classical statistical mechanics [5].

The ambiguity function of a signal whose complex envelope is denoted by $u(t)$ is defined as

$$|X(\tau,\nu)| = \left| \int_{-\infty}^{\infty} u(t)u^*(t+\tau)\exp(j2\pi\nu t)dt \right| , \tag{1}$$

where $(\cdot)^*$ represents the conjugate operator, $j=\sqrt{-1}$, $|\cdot|$ is the modulus of a complex number, τ and ν are the incremental delay and Doppler frequency shift respectively. Otherwise stated, it is closely related to the modulus of a matched filter output when the input is a Doppler shifted version of the original signal to which the filter is actually matched (see discussion in Section 2.4 of [1]). It follows that $|X(0,0)|$ coincides with the output when the input signal is matched to the nominal delay and Doppler of the filter; non-zero values of τ and ν indicate a target from other range and/or velocity.

Assuming that $u(t)$ has unitary energy, $|X(\tau,\nu)|$ complies with the following four relevant properties.

1) **Maximum Value Property.**

$$|X(\tau,\nu)| \leq |X(0,0)| = 1 , \tag{2}$$

the maximum value of the ambiguity function is reached for $(\tau,\nu)=(0,0)$ and is equal to 1.

2) **Unitary Volume Property.**

$$\int_{-\infty}^{\infty}\int_{-\infty}^{\infty} |X(\tau,\nu)|^2 \, d\tau d\nu = 1 , \tag{3}$$

the volume underneath the squared ambiguity function is unitary.

3) **Symmetry.**

$$|X(\tau,\nu)| = |X(-\tau,-\nu)| , \tag{4}$$

the ambiguity function shares a symmetry property about the origin.

4) **Linear Frequency Modulation (LFM) Property.**

If $|X(\tau,\nu)|$ is the ambiguity function corresponding to $u(t)$, then $|X(\tau,\nu-k\tau)|$ is the ambiguity function of $u(t)\exp(j\pi kt^2)$.

A more concise way of representing the ambiguity function consists of examining the one-dimensional zero-delay and zero-Doppler *cuts*. The cut of $|X(\tau,\nu)|$ along the delay axis is

$$|X(\tau,0)| = \left|\int_{-\infty}^{\infty} u(t)u^*(t+\tau)dt\right| = |R(\tau)|\,, \tag{5}$$

where $R(\tau)$ is the autocorrelation function of $u(t)$. The cut along the Doppler axis is

$$|X(0,\nu)| = \left|\int_{-\infty}^{\infty} |u(t)|^2 \exp(j2\pi\nu t)dt\right|\,, \tag{6}$$

which is independent of any phase or frequency modulation of the input signal. Further interesting properties of the ambiguity function can be found in [6]. Finally, in [1], the concept of periodic ambiguity function is presented and its connection with (1) is discussed.

III. Ambiguity Function of Basic Radar Signals

In this section, we present the ambiguity function of some basic signals (unmodulated rectangular pulse, LFM pulse, and coherent pulse train) [7][ch. 8] and discuss their suitability for radar applications.

A. Rectangular Pulse

The rectangular pulse of length t_p and unitary energy is given by[3]

$$u(t) = \frac{1}{\sqrt{t_p}}\text{rect}\left(\frac{t}{t_p}\right)$$

and the corresponding ambiguity function is

$$|X(\tau,\nu)| = \begin{cases} \left|\left(1-\dfrac{|\tau|}{t_p}\right)\dfrac{\sin[\pi t_p(1-|\tau|/t_p)\nu]}{\pi t_p(1-|\tau|/t_p)\nu}\right| = \left|\left(1-\dfrac{|\tau|}{t_p}\right)\text{sinc}\left[t_p(1-|\tau|/t_p)\nu\right]\right|, & |\tau| \le t_p\,, \\ 0 \qquad \text{elsewhere} \end{cases} \tag{7}$$

[3]The function rect(x) is equal to 1, if $|x| \le 1/2$, and is equal to 0 elsewhere. The function sinc(x) is defined as $\text{sinc}(x) = \dfrac{\sin(\pi x)}{\pi x}$.

In Figures 1a-1c, (7) is plotted together with the contours and the cuts along the delay and Doppler axes. Notice that (7) is limited to an infinite strip whose size on the delay axis is $2t_p$. As to the cut at $\tau = 0$, it exhibits the first nulls at $\nu_{null} = \pm\frac{1}{t_p}$ and, since the sinc$(\cdot)$ function has a peak sidelobe at -13.3 dB, the practical extension of the ambiguity function along the Doppler axis can be considered $2/t_p$.

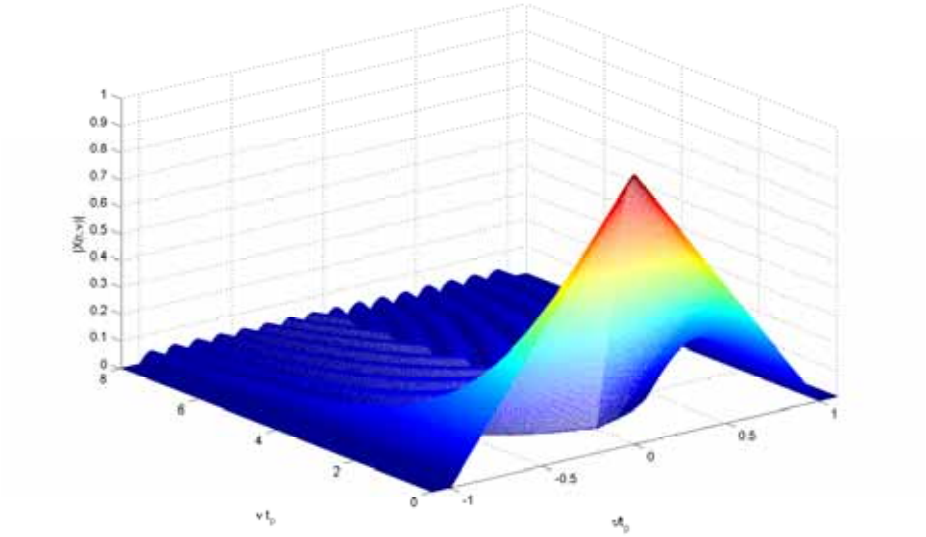

Figure 1a: Ambiguity function of an unmodulated rectangular pulse of length t_p.

In general, the rectangular pulse is not a desirable waveform from a pulse compression standpoint, because the autocorrelation function is too wide in time, making it difficult to discern multiple overlapping targets.

B. LFM Pulse

The LFM pulse or *chirp* is commonly used in radar and sonar applications. It has the advantage of greater bandwidth while keeping the pulse duration short and the envelope constant. The complex envelope of a LFM pulse, with instantaneous frequency $f(t) = kt$, is

$$u(t) = \frac{1}{\sqrt{t_p}}\text{rect}\left(\frac{t}{t_p}\right)\exp(j\pi kt^2)\,,$$

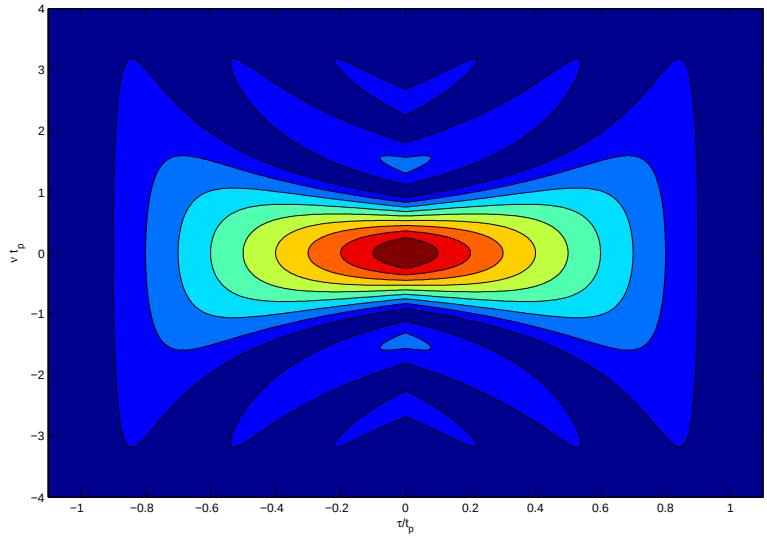

Figure 1b: Ambiguity function contours of an unmodulated rectangular pulse of length t_p.

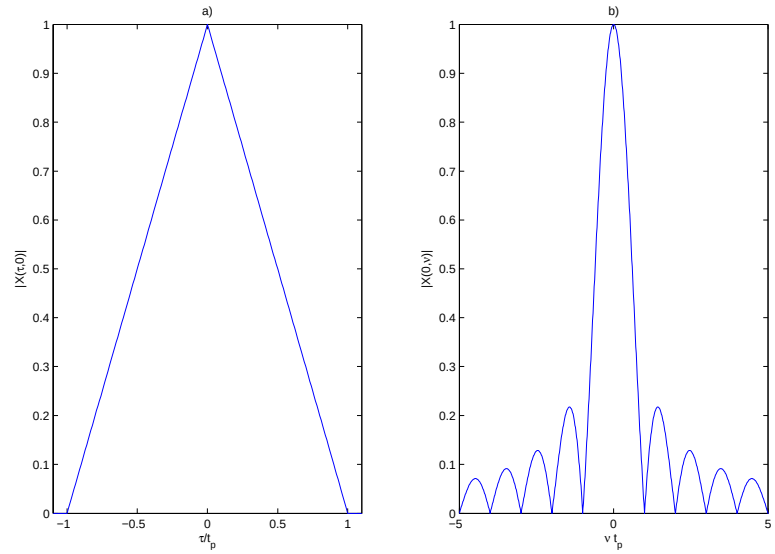

Figure 1c: Ambiguity function of an unmodulated rectangular pulse of length t_p. a) Zero-Doppler cut. b) Zero-delay cut.

and the corresponding ambiguity function is given by

$$|X(\tau,\nu)| = \begin{cases} \left|\left(1-\dfrac{|\tau|}{t_p}\right)\operatorname{sinc}\left[t_p(1-|\tau|/t_p)(\nu-k\tau)\right]\right|, & |\tau| \le t_p\,, \\ 0 \qquad \text{elsewhere} \end{cases} \tag{8}$$

In Figures 2a-2c, (8) is plotted together with the contours and the cuts along the delay and Doppler axes.

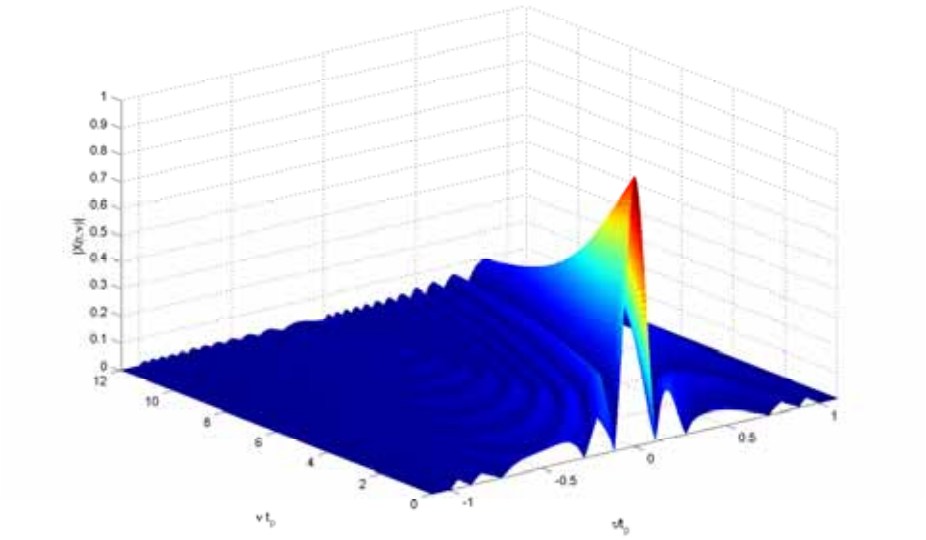

Figure 2a: Ambiguity function of a LFM rectangular pulse of length t_p and with $kt_p^2 = 10$.

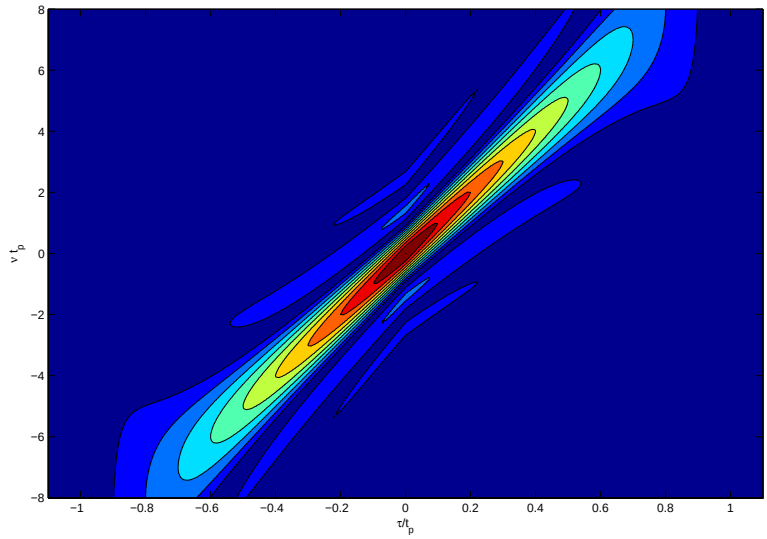

Figure 2b: Ambiguity function contours of a LFM rectangular pulse of length t_p and with $kt_p^2 = 10$.

Notice that the cut along the Doppler axis ($\tau = 0$) is the same as in Figure 1c-b. On the

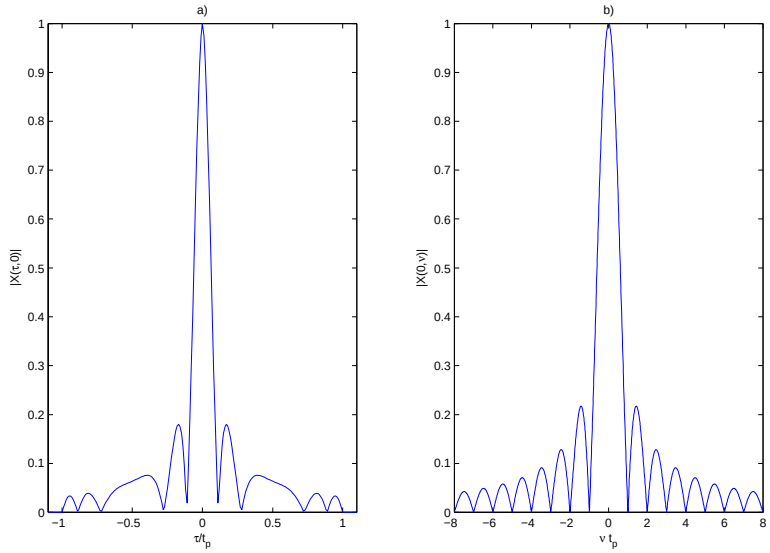

Figure 2c: Ambiguity function of a LFM rectangular pulse of length t_p and with $kt_p^2 = 10$. a) Zero-Doppler cut. b) Zero-delay cut.

contrary, the cut along the Delay axis ($\nu = 0$) is deeply different from Figure 1c-a: if $kt_p^2 = t_p \Delta f \gg 4$ (Δf is the total frequency deviation), it exhibits the first nulls at

$$\tau_{null} = \pm \frac{1}{kt_p} = \pm \frac{1}{\Delta f} .$$

This means that the *range window* has been compressed by a factor $D = t_p \Delta f$, which is usually referred to as compression ratio. Notice also that the ambiguity function volume is mainly concentrated on a diagonal ridge.

Slight Doppler mismatches for the LFM pulse do not change the general shape of the pulse and reduce the amplitude very little, but they appear to shift the pulse in time. Thus, an uncompensated Doppler shift changes the target's apparent range; this phenomenon is called range-Doppler coupling.

Finally, we just mention that non-linear FM pulses can be conceived (see for instance [8] and [1]).

C. Coherent Pulse Train

The complex envelope of a coherent pulse train, composed by N equally spaced pulses, can be written as

$$u(t) = \frac{1}{\sqrt{N}} \sum_{n=1}^{N} u_n(t - (n-1)T_R) \tag{9}$$

where T_R is the pulse repetition period and $u_n(t)$ is the complex envelope of the n-th unitary energy pulse. Assuming that the pulse train is uniform (i.e. $u_n(t) = u_C(t)$, $n = 1, \ldots, N$) and that the separation between pulses $T_R/2$ is greater than the pulse duration t_p, the ambiguity function of (9) can be expressed as

$$|X(\tau,\nu)| = \frac{1}{N} \sum_{p=-(N-1)}^{N-1} |X_C(\tau - pT_R, \nu)| \left| \frac{\sin[\pi\nu(N-|p|)T_R]}{\sin(\pi\nu T_R)} \right| , \qquad |\tau| \leq NT_R \, , \tag{10}$$

(zero elsewhere) with $|X_C(\tau,\nu)|$ is the ambiguity function of $u_C(t)$.

In Figure 3, we assume unmodulated rectangular pulses, $N = 6$, $T_R = 5t_p$ and plot (10) in the range-Doppler domain[4]. Due to its shape (10) is often referred to as *bed of nails*. The zero-Doppler cut shows that there are multiple triangular windows: the separation between two consecutive peaks is equal to the pulse repetition period T_R. Moreover, all the triangular windows have the same width $2t_p$, but their height decreases as the distance from the origin increases.

As to the cut for $\tau = 0$, there are multiple peaks spaced apart $1/T_R$ and $N - 2$ smaller sidelobes between them. The first nulls occur at $\nu = \pm 1/NT_R$, namely the width of the main peak (in Doppler) is ruled by the length of the Coherent Processing Interval (CPI).

IV. Coded Radar Signals

The ambiguity function of a coherent pulse train allows a main peak narrow both in range and in Doppler, but exhibits some peaks with almost the same amplitude as the main peak. These might be deleterious and can lead to range/Doppler ambiguities very difficult to resolve.

If we wish to maintain a very narrow main peak but cannot accept the additional peaks typical of the *bed of nails*, we can spread the volume in a low but wide pedestal around the main peak. This kind of ambiguity function is referred to as *thumbtack* shape and can be obtained considering coded radar signals.

[4]In the following, the MATLAB toolbox of [9] is used to plot the ambiguity functions.

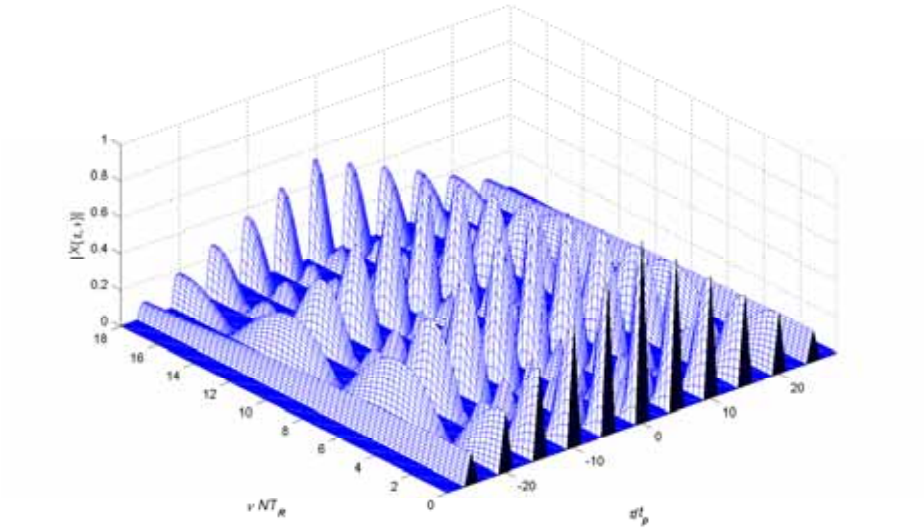

Figure 3: Ambiguity function of a coherent train of uniform pulses with $N = 6$, pulse length t_p, and pulse repetition period $T_R = 5t_p$.

A. Frequency Coding: Costas Sequences

The complex envelope of a frequency coded pulse of length t_p can be written as

$$u(t) = \frac{1}{\sqrt{N t_b}} \sum_{n=1}^{N} u_n(t - (n-1)t_b)\,, \tag{11}$$

where

$$u_n(t) = \begin{cases} \exp(j2\pi f_n t) & 0 \le t \le t_b \\ \\ 0 \qquad \text{elsewhere} \end{cases} \tag{12}$$

t_b is the length of each subpulse (time-slot duration, $N t_b = t_p$), the frequency shift in the n-th time slot is $f_n = a_n / t_b$, while the hopping (coding) sequence is

$$\{a_n\} = a_1, \ldots, a_N\,, \qquad a_n \in \{0, \ldots, N-1\}\,.$$

The frequency history of (11) can be represented through the coding matrix (Table I) where the horizontal axis, representing time, is divided in N time-slots of length t_b and the vertical axis is used to represent equally spaced frequencies. The (h, k)-th entry of the binary matrix can assume only two values: 1 if the h-th frequency is transmitted in the k-th time slot, 0 elsewhere. Obviously, there is only a 1 per column.

0	1	0	0	0	0	0
0	0	0	1	0	0	0
0	0	0	0	1	0	0
1	0	0	0	0	0	0
0	0	0	0	0	0	1
0	0	0	0	0	1	0
0	0	1	0	0	0	0

Frequency

Time

Table I: Binary matrix representation of frequency coding.

The corresponding ambiguity function can be evaluated through the expression

$$|X(\tau,\nu)| = \frac{1}{N}\left|\sum_{m=1}^{N}\exp(j2\pi(m-1)\nu t_b)\left[\Phi_{mm}(\tau,\nu)+\sum_{n=1,m\neq n}^{N}\Phi_{mn}(\tau-(m-n)t_b,\nu)\right]\right| \tag{13}$$

where

$$\Phi_{mn}(\tau,\nu) = \begin{cases} \left(1-\dfrac{|\tau|}{t_b}\right)\operatorname{sinc}(\alpha_{mn})\exp(-j\beta_{mn}-j2\pi f_n\tau), & |\tau|\leq t_b\,, \\ 0 \qquad \text{elsewhere} \end{cases} \tag{14}$$

and

$$\begin{aligned} \alpha_{mn} &= (f_m - f_n - \nu)\,(t_b - |\tau|) \\ \beta_{mn} &= \pi\,(f_m - f_n - \nu)\,(t_b + \tau)\ . \end{aligned}$$

Slightly different codes can strongly affect the ambiguity function of the signal; hence it is of interest to present a methodology which roughly predicts the ambiguity shape. Such a technique is based on the observation that the cross correlation between signals at different frequencies approaches zero when the frequency difference is large with respect to the inverse of the signal duration (or equal to multiples of that inverse). The prediction is possible overlaying a copy of the binary matrix on itself, and then shifting one relative to the other according to the desired delay (horizontal shifts) and Doppler (vertical shifts). A coincidence of two elements in the matrix denotes a peak of amplitude one in the predicted ambiguity function, two coincidences

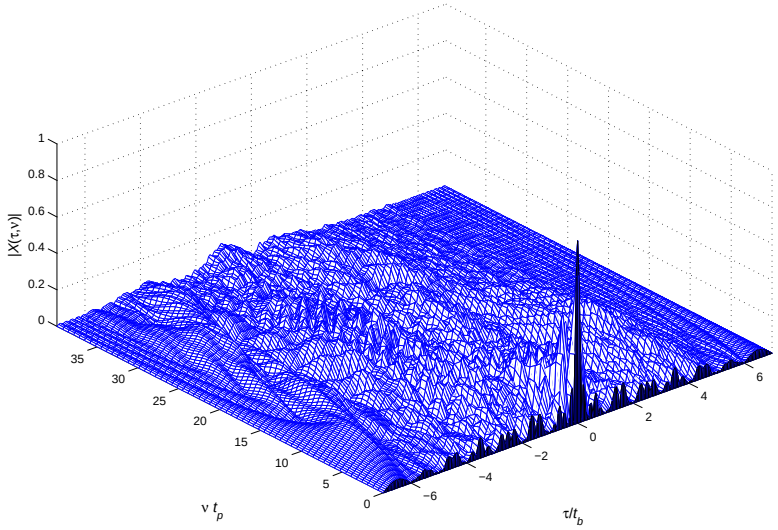

Figure 4a: Ambiguity function of a Costas signal with coding sequence $(3,\ 6,\ 0,\ 5,\ 4,\ 1,\ 2)$.

a peak of amplitude 2, and so on. The maximum number of coincidences is the number of frequencies (N in our example), and can be reached only in the origin (zero delay and zero Doppler). Normalizing the maximum peak at 1, we can assume a coincidence equal to a peak of amplitude $\dfrac{1}{N}$.

Definition 1. A coding sequence is a Costas code [10] if all the non-zero shifts of the binary matrix do not lead to more than one coincidence.

In Figure 4a, we plot the ambiguity function of a Costas coded pulse with $N = 7$ and coding sequence $(a_1, \ldots, a_N) = (3,\ 6,\ 0,\ 5,\ 4,\ 1,\ 2)$. The thumbtack nature of the ambiguity function is clearly evident. Moreover, in Figure 4b, we plot the contours of (13) for $|X(\tau, \nu)| = 0.125$. Notice that there is a similarity between Figure 4b and the sidelobe matrix [1, p. 77] of the coding sequence (Table II). In Figure 4c, we plot the autocorrelation function (zero-Doppler cut) : as expected, there are nulls at $\tau = kt_b$. Moreover, according to Property 4 of the ambiguity function, we do not need to plot the zero-delay cut, since it does not depends on the frequency modulation, but only on the magnitude of the unmodulated pulse.

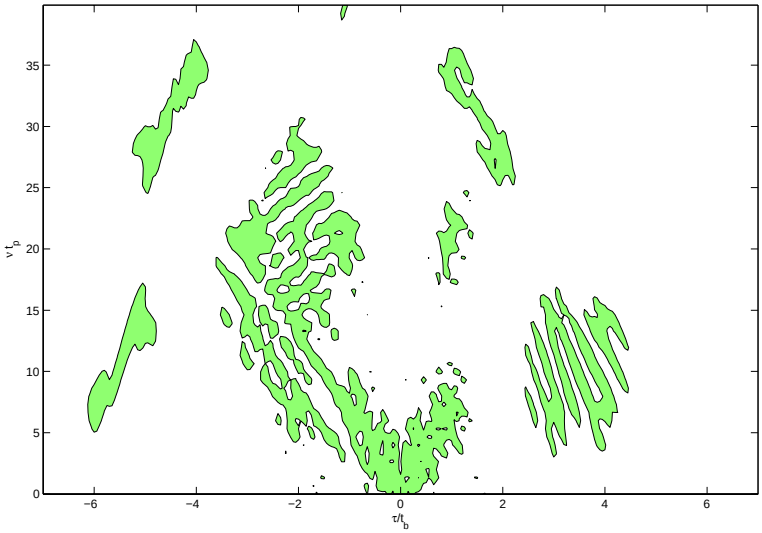

Figure 4b: Ambiguity function contours at 0.125 of a Costas signal with coding sequence $(3,\ 6,\ 0,\ 5,\ 4,\ 1,\ 2)$.

Sidelobe matrix

Doppler													
6	0	0	0	0	0	1	0	0	0	0	0	0	0
5	0	0	1	0	0	0	0	1	0	0	0	0	0
4	0	1	0	0	1	0	0	0	1	0	0	0	0
3	0	0	0	1	1	1	0	1	0	0	0	0	0
2	0	1	0	1	1	0	0	0	0	1	1	0	0
1	1	0	0	0	1	1	0	1	0	1	1	0	0
0	0	0	0	0	0	0	7	0	0	0	0	0	0
	-6	-5	-4	-3	-2	-1	0	$+1$	$+2$	$+3$	$+4$	$+5$	$+6$

Delay

Table II: Sidelobe matrix of a Costas signal with coding sequence $(3,\ 6,\ 0,\ 5,\ 4,\ 1,\ 2)$.

Unfortunately, it does not exist a constructive procedure to determine all the possible Costas sequences of a fixed length, nor how many they are. To circumvent this drawback, two approaches can be followed.

- An exhaustive search among all the $N!$ possible sequences of length N;
- A constructive procedure to determine a subclass of particular Costas sequences.

The first method needs grid computing, and cannot provide very long sequences. For example, using a grid of more than 700 processors, a complete search of Costas array of length 30

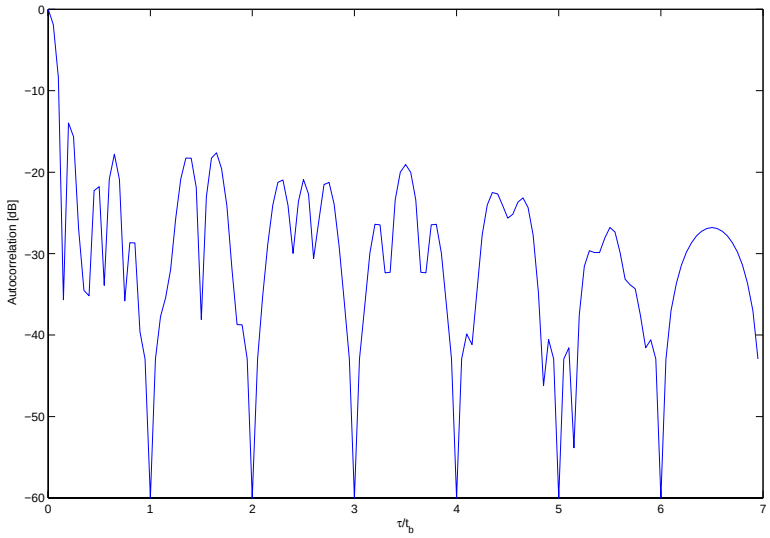

Figure 4c: Autocorrelation function of a Costas signal with coding sequence $(3,\ 6,\ 0,\ 5,\ 4,\ 1,\ 2)$.

requires more than 4 years [11]. Actually, the public database of Costas arrays contains all the sequences starting from the unique sequence of length 1, up to the 204 sequences of length 27 [11]. Moreover, the ratio between the number of length N Costas sequences and the $N!$ possible sequences, decreases very quickly [11], namely it is even more difficult to find a Costas sequence increasing the length.

A different construction technique is based on the theory of Galois finite fields[5]. Starting from a primitive element of $GF(N)$, i.e. an element of the field that can generate all the others elements but for 0, it is possible to conceive several procedures to construct a Costas sequence. The most used techniques are the *Welch 1*, the *Welch 2*, the *Golomb 2*, the *Lempel 2*, and the *Taylor 4*. Let us now illustrate how the *Welch 1* procedure can be implemented.

Choose a length $N > 3$ such that $N = p - 1$, where p is a prime number. Find a primitive element α of $GF(p)$. Numbering the columns of the array in Table III with $k = 0, 1, 2, \ldots, p-2$ and the rows with $h = 1, 2, \ldots, p-1$, we put a 1 in position (h, k) if and only if $h = \alpha^k$ (mod p). For example, let us consider $N = 4$, so $p = 5$. A primitive element of $GF(5)$ is 2, since the elements $\{1, 2, 3, 4\}$ can be obtained as $\{2^0, 2^1, 2^3, 2^2\}$ (mod p). Now, we can construct the

[5]In the following, a Galois field containing the elements from 0 to $N-1$ will be denote by $GF(N)$.

following matrix

Frequency \ Time	0	1	2	3
1	1	0	0	0
2	0	1	0	0
3	0	0	0	1
4	0	0	1	0

Table III: *Welch I* construction matrix.

which provides the Costas code $(1,\ 2,\ 4,\ 3)$.

Finally, in Table IV, we present a short list of procedures, which can be used to obtain Costas sequences whose length ranges between 3 and 30 [12].

Order	Working constructions	Order	Working constructions
–	–	16	T_1, W_1, W_3, L_3, G_3
–	–	17	T_0, W_2, L_2, G_2
3	T_1, W_2, L_2, G_2	18	W_1
4	T_1, W_1, G_3, G_4, G_5	19	W_0
5	$T_0, W_2, L_2, T_4, G_2, G_3, G_4$	20	G_3
6	T_1, W_3, L_2, G_2, G_3	21	W_2, L_2, G_2
7	W_0, L_2, T_4, G_2	22	T_1, W_1, G_3
8	T_1, W_3, L_3, G_3	23	T_0, L_2, G_2
9	W_2, L_2, G_2	24	G_3
10	T_2, W_1, W_3, L_3, G_3	25	L_2, G_2
11	T_0, W_2, L_2, G_2	26	W_3, L_2, G_2
12	W_1, G_4	27	W_2, L_2, T_4, G_2
13	W_0, G_3	28	T_1, W_1, G_3, G_4
14	L_2, G_2, G_3	29	T_0, W_2, L_2, G_2, G_3
15	W_2, L_2, T_4, G_2	30	W_3, L_2, G_2

Table IV

Constructions that successfully produce Costas arrays of order ≤ 30 T_i Taylor i-th procedure.

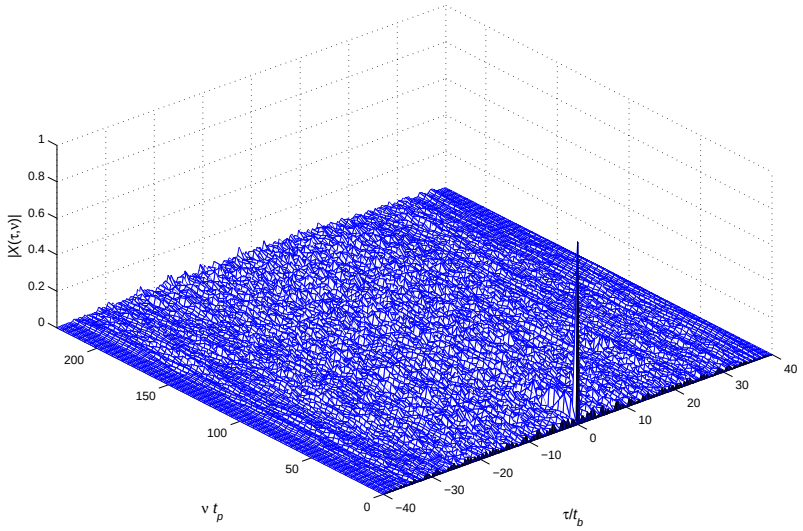

Figure 5: Ambiguity function of a Costas sequence of length 40.

W_i Welch i-th procedure. G_i Golomb i-th procedure. L_i Lempel i-th procedure.

The ambiguity function behavior of the Costas coding is more pronounced for long sequences. In Figure 5, we plot the ambiguity function of a Costas sequence of length 40 [1]. This last example of a relatively long Costas signal indicates that the longer the sequence, the closer its ambiguity function to the thumbtack shape. Regarding the zero-Doppler cut, the sidelobes are usually below -26 dB. However, the near sidelobes $(t_b/N < \tau < t_b)$ are higher, decaying from -13.7 dB in a manner typical of the autocorrelation function sidelobes of a signal with a rectangular spectrum. Indeed, the spectrum of our relatively long Costas signal is nearly rectangular.

B. Frequency Coding: Pushing Sequences

This class of frequency coded signals has been introduced by Chang and Bell in [13].

Definition 2. For the ambiguity function of a frequency coded waveform, a *clear area of size s* is a connected area centered at the origin of the (τ, ν)-plane, where $|\tau| < st_b$ and $|\nu| < s/t_b$, such that no sidelobe peaks (of height greater than $1/N$) are present in this area.

A frequency-coding sequence having the ambiguity function with a clear area of size s is called a pushing sequence with power s, where $s \geq 1$.

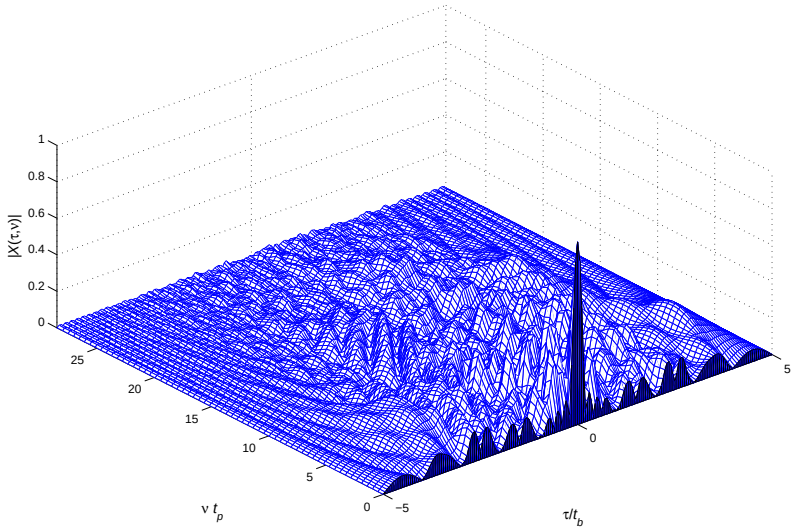

Figure 6a: Ambiguity function of a Costas-pushing sequence of length 5.

Of particular relevance are the codes which are both Costas and pushing (Costas-pushing sequences). They share some interesting symmetry properties (Group D_4 Dihedral Symmetry Property) [13] which permit to derive more pushing-Costas sequences from a given one. Moreover a Costas sequence, derived from the *Taylor 4* (T_4) construction, is also a pushing sequence of power 1.

In Figures 6a-6b, we plot the ambiguity function and the contours at $|X(\tau,\nu)| = 0.1667$ of a Costas-pushing coded pulse with $N = 5$ and coding sequence $(a_1,\ldots,a_N) = (1,\,3,\,0,\,4,\,2)$. The clear area and the thumbtack nature of the ambiguity function can be directly seen from the figures.

C. Phase-Coded Radar Signals

A pulse of duration t_p is divided into N bits (chips) of identical duration $t_b = t_p/N$ and each of them is *coded* with a different pulse value. The complex envelope of the phase-coded pulse is given by

$$u(t) = \frac{1}{\sqrt{t_p}} \sum_{n=1}^{N} u_n \text{rect}\left[\frac{t-(n-1)t_b}{t_b}\right. \tag{15}$$

where $u_n = \exp(j\phi_n)$ and the set of N phases $\{\phi_1,\phi_2,\ldots,\phi_N\}$ is the *phase code* associated with $u(t)$. Criteria for selecting a specific code are the resolution properties of the resulting waveform

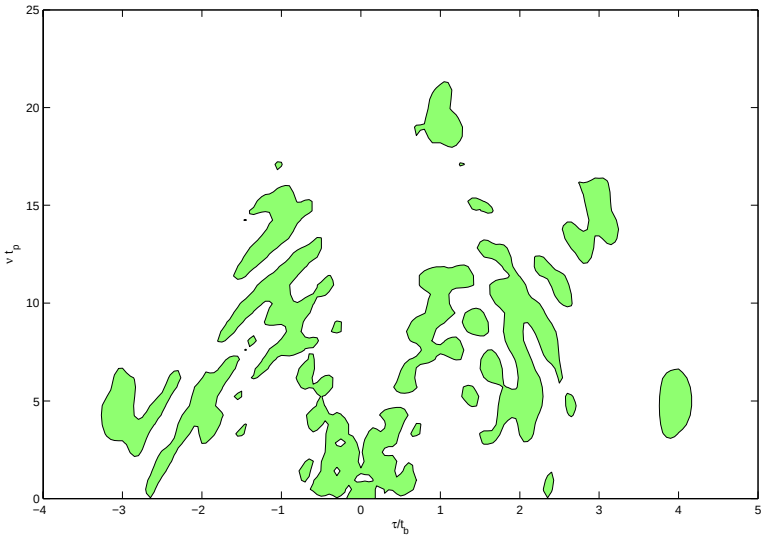

Figure 6b: Ambiguity function contours at 0.1667 of a Costas-pushing signal with code sequence $(1,\ 3,\ 0,\ 4,\ 2)$.

(shape or ambiguity function), frequency spectrum and the ease through which the system can be implemented. However, finding a code which leads to a predetermined range-Doppler resolution is very complicated; choosing a code ensuring a good autocorrelation function is easier.

The autocorrelation function of a phase-coded pulse is a continuous function of the delay τ. The properties of the autocorrelation function should be examined, in general, for all $-t_p < \tau < t_p$. It can be shown [1, pp. 101 - 102] that it is sufficient to calculate the correlation function at integer multiples of the bit duration. The other can obtained connecting the values at $\tau = kt_b$ using straight lines in the complex plane. Thus, the optimization of the *continuous* autocorrelation peaks is simplified to the minimization of the *discrete* correlation function $|R_k|$ values [1].

1) Barker codes: The *Barker* codes [14] were designed as the sets of N binary pulses yielding a peak-to-peak sidelobe ratio equal to N. In [14] and [15] all the known binary sequences complying with this property are reported. It has been shown that no Barker codes exist for $13 < N < 1.898.884$ and for all odd $N > 13$ [16]. In Figure 7a the autocorrelation function of a phase coded pulse using a Barker code of length $N = 13$ is shown. In Table V, all the known binary Barker codes are reported.

One of the main drawbacks of the Barker codes is that they are optimized only for the

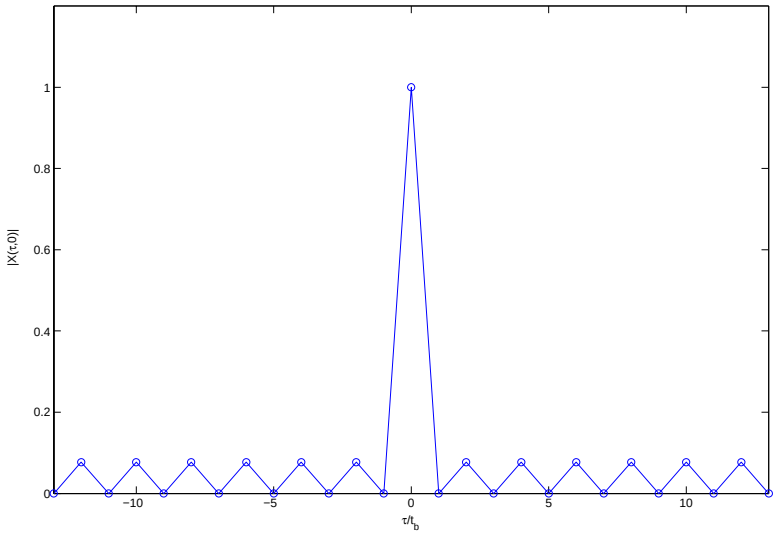

Figure 7a: Autocorrelation function of a phase-coded pulse using the 13-element Barker code.

Code length	Code
2	11 or 10
3	110
4	1110 or 1101
5	11101
7	1110010
11	11100010010
13	1111100110101

Table V

All known binary Barker codes.

autocorrelation function, i.e. the chosen peak-to-peak sidelobe ratio is valid only for the zero-Doppler cut. Thus, if the target return is Doppler shifted the sidelobe peaks are greater than those expected. Otherwise stated, Barker codes exhibit a low Doppler tolerance. Figure 7b shows the ambiguity function of a 13-element Barker code; notice that the sidelobe peaks are higher than $1/N$ for many values of the Doppler shift and the main peak is lower than 1 for those Doppler

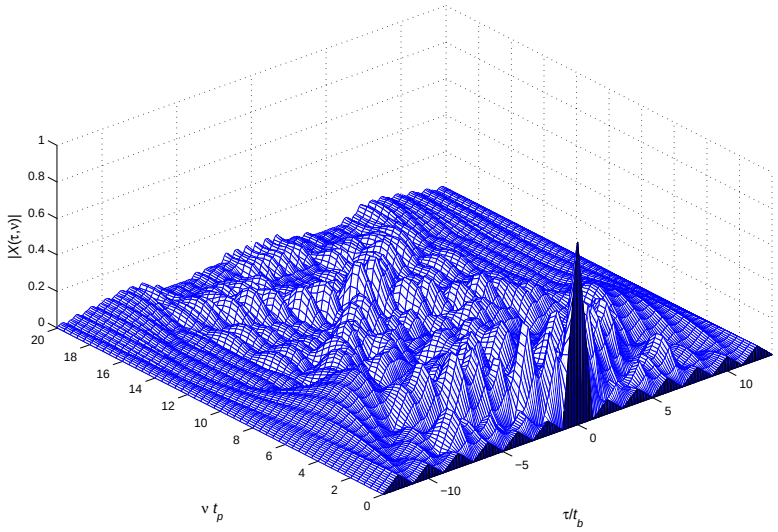

Figure 7b: Ambiguity function for a 13-element Barker code.

values.

2) Polyphase Barker Codes: The Barker codes are limited by the binary assumption. Allowing any phase value can lead to lower sidelobes. In this way, a *polyphase* code is realized. The polyphase N-sequence with minimal peak-to-sidelobe ratio excluding the outermost sidelobe (which is always $1/N$, both for binary and polyphase codes) is called *generalized Barker sequence* or *polyphase Barker sequence*. Actually, systematic methods to produce polyphase Barker sequences are not yet found; using numerical optimization techniques allow to search such codes without restrictions on the values of the sequence phases. Figure 8, shows the autocorrelation function magnitude for the 13-element polyphase Barker code. Notice that the peak sidelode, whose magnitude is $1/N$, is located at $\tau = \pm 12 t_b$.

3) Frank Codes and extensions: The *Frank* code [17] is derived from the phase history of a linearly frequency stepped pulse; the Frank code is designed to ensure low sidelobe peaks even for non zero-Doppler values. However, it applies only for a square code length ($N = L^2$). The

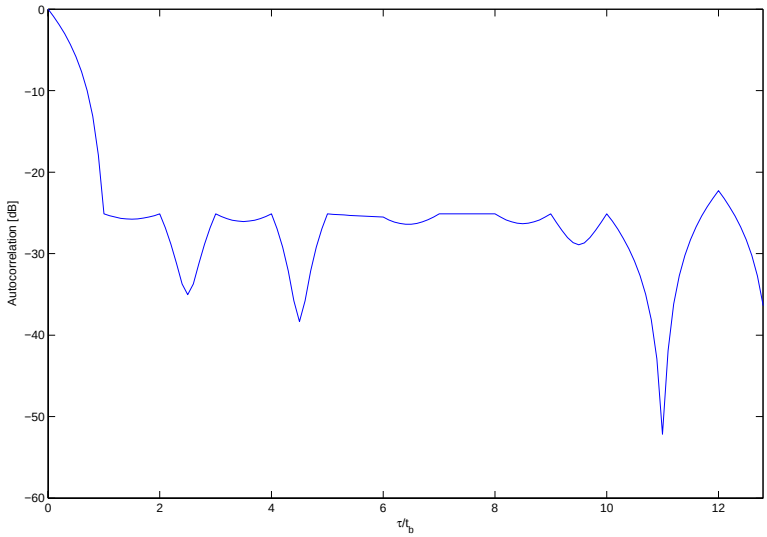

Figure 8: Autocorrelation function of 13-element polyphase Barker code.

elements $u_n\,(1 \leq n \leq N)$ of a $N = L^2$ Frank code are

$$u_{(n-1)L+k} = \exp(j\phi_{n,k}) \qquad 1 \leq n \leq L \qquad 1 \leq n \leq L \tag{16}$$

where $\phi_{n,k} = 2\pi(n-1)(k-1)/L$. The phase values in (16) can be obtained from the elements of the $L \times L$ discrete matrix

$$\begin{bmatrix} 0 & 0 & 0 & \dots & 0 \\ 0 & 1 & 2 & \dots & L-1 \\ 0 & 2 & 4 & \dots & 2(L-1) \\ \vdots & \vdots & \vdots & \ddots & \vdots \\ 0 & (L-1) & 2(L-1) & \dots & (L-1)^2 \end{bmatrix},$$

concatenating the rows and multiplying for $2\pi/L$; finally, the phase values are taken mod 2π. Frank code shares two important properties [1]:

1) it is perfect[6];

[6]A phase code having zero periodic autocorrelation sidelobes is called *perfect*.

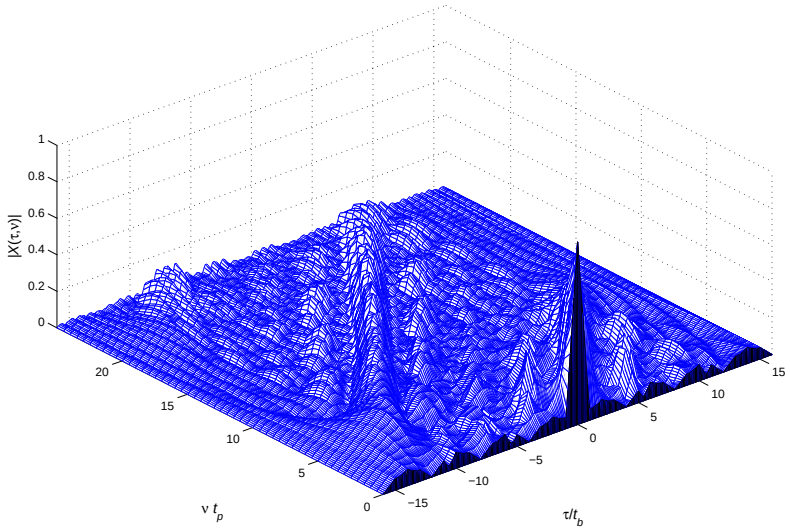

Figure 9: Ambiguity function of 16-element Frank code.

2) the autocorrelation function exhibits relatively low sidelobes.

Figure 9 shows the ambiguity function for a 16-elements Frank code.

The Frank code can be modified into the P1, P2 and PX codes, with the dc frequency[7] term in the middle of the pulse instead of the beginning; also the modified versions can be applied only for square code length, i.e. $N = L^2$. The PX code [18] yields the same aperiodic peak sidelobe as the Frank code, but ensures a low integrated sidelobe level. The elements of the PX code are defined as

$$s_{(n-1)L+k} = \exp(j\phi_{n,k}) \qquad 1 \leq n \leq L \qquad 1 \leq k \leq L \tag{17}$$

where

$$\phi_{n,k} = \begin{cases} \dfrac{2\pi}{L}\left(\dfrac{L+1}{2} - k\right)\left(\dfrac{L+1}{2} - n\right) & L \quad \text{even} \\ \\ \dfrac{2\pi}{L}\left(\dfrac{L}{2} - k\right)\left(\dfrac{L+1}{2} - n\right) & L \quad \text{odd}\,. \end{cases} \tag{18}$$

In the same way as for the Frank code, it is possible to derive a matrix to form the phase values for the PX code.

[7]The dc frequency term is in correspondence to the zero-phase value in the code.

P2 code [19]-[20] can be constructed only for L even and is defined exactly as the PX code. This code is palindromic as it exhibits some specific symmetry properties [1]. P1 code [19]-[20] elements are defined using (17) where

$$\phi_{n,k} = \frac{2\pi}{L}\left(\frac{L+1}{2} - n\right)\left[(n-1)L + (k-1)\right]. \tag{19}$$

The P1 code, unlike PX and P2 codes, is perfect, as the Frank code. The ambiguity function of the P1 code for odd L is identical to that of the Frank code. For even L, the ambiguity functions of P2 and PX codes are very similar to the one of the P1 code and also to the one of the Frank code.

D. A Table with Some Common Radar Codes

There exist further coding strategies, different from those presented in the previous sub-sections. The interested reader can consult the excellent book of Levanon and Mozeson [1] for a more complete description. Here, we just provide a table (Table VI, of course not exhaustive) to summarize some common radar codes [21]-[35].

Name	Inventor	Year	Type
Barker Code	R.H. Barker	1953	Phase Codes
Complementary Code	R. Sivaswamy	1978	Complementary Phase Codes
Huffmann Code	D.A. Huffmann	1962	Amplitude Phase Codes
Frank Code	R.L. Frank, S.A. Zadoff	1962	Chirplike Phase Codes
Zadoff-Chu Code	S.A. Zadoff	1963	Chirplike Phase Codes
Gold Code	R. Gold	1967	Phased Code based on binary sequence
Minimum Peak Sidelobe code	J. Lindner, N. Cohen et al.	1975	Binary Phase Codes
Welti Code	G.R. Welti	1960	Quaternary Code
P1 and P2 Codes	B.L. Lewis, F.F. Kretschmer	1981	Phase Codes
P3 qnd P4 Codes	B.L. Lewis, F.F. Kretschmer	1982	Phase Codes
Costas Array	J.P. Costas	1984	Frequency Codes
Quadratic congruential coding	J.R. Bellegarda, E.L. Titlebaum	1991	Frequency Codes
Polyphase Barker Codes	L. Bomer, M. Autweiler	1989	Phase Codes
Generalized P4 Code	F.F. Kretshmer, K. Gerlach	1991	Phase Codes
Biphase Perfect Code	S.W. Golomb	1992	Biphase Codes
Ipatov	V.P. Ipatov	1992	Codes with minimal peak response loss
P(n,k)	T. Felhauer	1994	Phase Codes
Px Code	P.B. Rapajic, R.A. Kennedy	1998	Phase Codes
PONS based Complementary code	P. Zulch, M. Wicks, et al.	2002	Complementary Codes
Orthogonal Codes	N. Levanon, E. Mozeson	2003	Train of Orthogonal Coded Pulses
Multicarrier Phase Coded Pulse	N. Levanon, E. Mozeson	2002	Multicarrier Phase Radar Signals

Table VI

Typical codes and their inventors.

V. Coherent Train of Diverse Pulses

With reference to a train of coherent pulses, quite often, in practice, the pulses are modulated and are not identical. Modulation produces a wider bandwidth, hence pulse compression. Moreover, diversity between the pulses of the train can be exploited to obtain advantages such as lower delay sidelobes or lower recurrent lobes. The addition of a modulation, keeping the pulses identical, leads to an analytic expression for the ambiguity function. Adding a diversity in amplitude or diverse modulations in the pulses usually requires a numerical analysis (but for in some simple cases), since the ambiguity function is only available as an integral function.

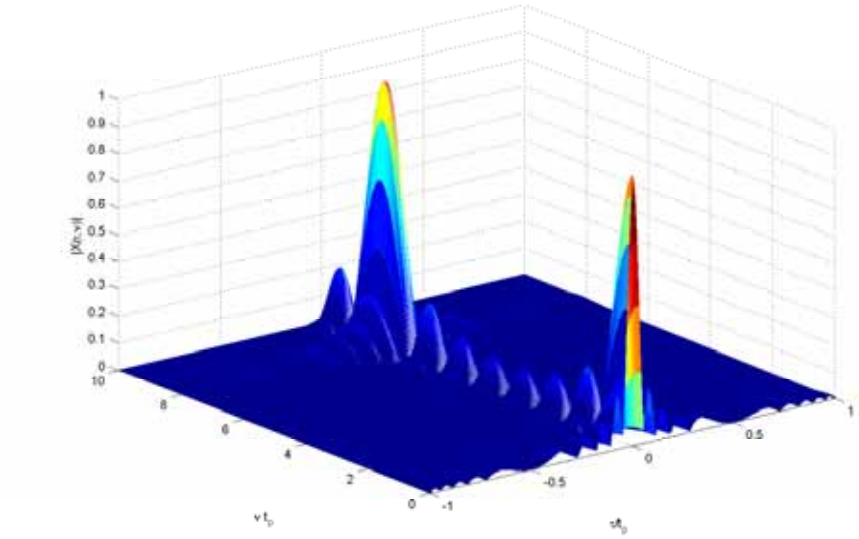

Figure 10: Partial ambiguity function ($|\tau| \leq t_p$) of a coherent uniform train of eight LFM pulses $kt_p^2 = 20$, and $T_R = 9t_p$.

A train of identical LFM pulses provides both a good range and a good Doppler resolution (probably the most used radar signal in airborne applications). However, its ambiguity function (Figure 10) still presents significant sidelobes both in delay and in Doppler.

Performing an interpulse amplitude weighting permits to reduce the Doppler sidelobes at the price of a larger Doppler main lobe (at $\nu = 0$) and recurrent lobes. Similarly, an intrapulse weighting in LFM mitigates range sidelobes. The aforementioned weightings can be thus combined to reduce both range and Doppler sidelobes.

Another method for diversifying the identical pulse train relies on staggering the Pulse Repetition Frequency (PRF) obtaining a mitigation of the blind speeds problem.

Exploiting a pulse-to-pulse diversity can lead to:

- a reduction in the height of the recurrent (range) lobes of the autocorrelation function (i.e. around $\tau = nT_R$, $n = \pm 1, \pm 2, \ldots$);
- a reduction of near range sidelobes (i.e. around $|\tau| \leq t_p$);
- an increase in the overall bandwidth of the signal while maintaining relatively narrow instantaneous bandwidth.

In this context we mention the stepped-frequency pulse train (which consists of adding a frequency step Δf between consecutive pulses) as an efficient way to obtain large overall bandwidth (hence improved range resolution), while maintaining relatively narrow instantaneous bandwidth [36]. Moreover, a careful selection of the frequency stepping and LFM slopes can possibly

eliminate the ambiguous peaks of the autocorrelation function [37]-[38] (of course complying with the unitary volume constraint).

VI. CONCLUSIONS

In this lecture, we have presented an overview of the basic theory of radar waveforms. First of all, we have provided the concept of ambiguity function and have discussed its relevant properties. Then, we have reviewed the most common radar signals together with their ambiguity functions. The effects of a possible signal coding has been described: a special attention has been deserved to the class of frequency coded waveforms through a Costas sequence. Their construction, relying upon the theory of Galois fields, as well as the desirable properties deriving from the use of a Costas-pushing sequence are discussed. In the last part of the lecture, we have considered coherent pulse trains of diverse pulses and have discussed the effects of modulating the different parameters of the train.

Before concluding, we highlight that one of the trade-offs in radar signal design is between constant modulus and ambiguity function sidelobes. Efficient RF power amplifiers are presently operating at saturation and do not allow linear changes in amplitude. On the other hand, sidelobe reduction in range or Doppler usually require amplitude variations (weighting).

Another conflict involving a linear power amplifier relates variable amplitude and spectrum. The spectrum of constant amplitude pulse signal exhibits sidelobes which decay very slowly. Such behavior may often violate spectrum emission regulations and can possibly cause interference to neighboring radars and/or other telecommunication apparatus. On the contrary, suitable variable amplitude pulses are characterized by a rapid decay of the spectral tails.

Further radar waveforms with variable amplitude are the Huffman-coded signal and the multicarrier signals [1]. These two examples show that removing the constant amplitude restriction provides signals with additional degrees of freedom which can be exploited to further optimize the system performance.

Acknowledgements

The authors gratefully acknowledge Ing. S. De Nicola and Dr. L. Landi, for careful reading of the manuscript and useful suggestions, and Prof. N. Levanon for some interesting discussions on radar frequency coding.

REFERENCES

[1] N. Levanon and E. Mozeson, *Radar Signals*, John Wiley & Sons, 2004.

[2] C. E. Cook, and M. Bernfeld, *Radar Signals: An Introduction to Theory and Application*, Academic Press, New York, 1967.

[3] L. Falk, "From 'Information Theory in Radar - A Tribute to P. M. Woodward'", *Swedish Defence Research Agency*, Edinburgh, November 2004.

[4] J. Ville, "Theory and applications of the notion of complex signal", translated by I. Seline in *RAND Tech. Rpt. T-92*, RAND Corp., August 1958.

[5] E. Wigner, "On the quantum correction for thermodynamic equilibrium," *Physical Review*, Vol. 40, No. 5, pp. 749-759, June 1932.

[6] A. W. Rihaczek, *Principles of High Resolution Radar*, McGraw-Hill, New York, 1969.

[7] M. I. Skolnik, *Radar Handbook*, McGraw-Hill, New York, 2008.

[8] A. Di Vito, A. Farina, G. Fedele, G. Galati, and F. A. Studer, "Design of waveforms for long range radars," *Rivista Tecnica Selenia*, Vol. 9, No. 2, 1984.

[9] E. Mozeson and N. Levanon, "MATLAB Code for plotting ambiguity functions", *IEEE Trans. on Aerospace and Electronic Systems*, Vol. 38, No. 3, pp. 1064-1068, July 2002.

[10] J. P. Costas, "A study of a class of detection waveforms having nearly ideal range-Doppler ambiguity properties," *Proceedings of the IEEE*, Vol. 72, No. 8, pp. 996-1009, August 1984.

[11] K. Drakakis, "A review of Costas arrays," *Journal of Applied Mathematics*, Vol. 2006, No. 1, pp. 1-32, March 2006.

[12] S. W. Golomb and H. Taylor, "Constructions and properties of Costas arrays," *Proceedings of the IEEE*, Vol. 72, No. 9, pp. 1143-1163, September 1984.

[13] Chieh-Fu Chang and M.R. Bell, "Frequency coded waveforms for enhanced delay-Doppler resolution", *Proceedings of the IEEE Radar Conference 2002*, 22-25 April, pp.160-167.

[14] R. H. Barker, "Group synchronization of binary digital systems" in *W. Jackson (ed.), Communication Theory*, Academic Press, London, pp. 273-287, 1953.

[15] R. Turyn, "On Barker codes of even length", *Proceedings of the IEEE*, Vol. 51, No. 9, p. 1256, September 1963.

[16] S. Eliahou and M. Kervaire, "Barker sequences and difference sets", *L'Enseignement Mathematique*, Vol. 38, No. 3-4, pp. 345-382, 1992.

[17] R. L. Frank, "Polyphase codes with good non-periodic correlation properties", *IEEE Trans. on Information Theory*, Vol. 9, No. 1, pp. 43-45, January 1963.

[18] P. B. Rapajic and R. A. Kennedy, "Merit factor based comparison of new polyphase sequencies", *IEEE Communication Letters*, Vol. 2, No. 10, pp. 269-270, October 1998.

[19] B. L. Lewis and F. F. Kretschmer, "A new class of polyphase compression codes and techniques", *IEEE Trans. on Aerospace and Electronic Systems*, Vol. 17, No. 3, pp. 364-372, May 1981.

[20] B. L. Lewis and F. F. Kretschmer, "Corrections to: A new class of polyphase compression codes and techniques", *IEEE Trans. on Aerospace and Electronic Systems*, Vol. 17, No. 5, p. 726, September 1981.

[21] M. J. E. Golay, "Complementary series", *IRE Trans. on Information Theory*, Vol. 7, pp. 82-87, April 1961.

[22] D. A. Huffman, "The generation of impulse-equivalent pulse trains", *IRE Trans. on Information Theory*, Vol. 8, pp. 10-16, September 1962.

[23] S. A. Zadoff, "Phase coded communication system", *U.S. patent 3,099,796*, 30 July 1963, .

[24] R. Gold, "Optimal binary sequences for spread spectrum multiplexing," *IEEE Trans. on Information Theory*, Vol. 13, No.5, pp.619-621, October 1967.

[25] J. Lindner, "Binary sequences up to length 40 with best possible autocorrelation function", *Electronics Letters*, Vol. 11, No. 21, p. 507, October 1975.

[26] R. Sivaswamy, "Digital and analog subcomplementary sequences for pulse compression", *IEEE Trans. on Aerospace and Electronic Systems*, Vol. 14, No.2, pp. 343-350, March 1978.

[27] J. R. Bellegarda and E. L. Titlebaum, "Time-frequency hop codes based upon extended quadratic congruences", *IEEE Trans. on Aerospace and Electronic Systems*, Vol. 24, No. 6, pp. 726-742, November 1988.

[28] M. N. Cohen, J. M. Baden, and P. E. Cohen, "Biphase codes with minimum peak sidelobes", *Proceedings of the IEEE National Radar Conference 1989*, 29-30 March, pp. 62-66.

[29] L. Bomer and M. Antweiler, "Polyphase Barker sequences", *Electronics Letters*, Vol. 25, No. 23, pp. 1577-1579, November 1989.

[30] M. N. Cohen, M. R. Fox, and J. M. Baden, "Minimum peak sidelobes pulse compression codes", *Proceedings of the IEEE International Radar Conference 1990*, 7-10 May, pp. 633-638.

[31] F. F. Kretschmer and K. Gerlach, "Low sidelobe radar waveforms derived from orthogonal matrices", *IEEE Trans. on Aerospace and Electronic Systems*, Vol. 27, No. 1, pp. 92-102, January 1991.

[32] S. W. Golomb, "Two-valued sequences with perfect periodic autocorrelation", *IEEE Trans. on Aerospace and Electronic Systems*, Vol. 28, No. 2, pp. 383-386, March 1992.

[33] V. P. Ipatov, "Periodic discrete signals with optimal correlation properties", translated in ISBN 5-256-00986-9, available from the University of Adelaide, Australia.

[34] T. Felhauer, "Design and analysis of new P(n, k) polyphase pulse compression codes", *IEEE Trans. on Aerospace and Electronic Systems*, Vol. 30, No. 3, pp. 865-874,July 1994.

[35] P.A. Zulch, M.C. Wicks, B. Moran, S. Suvorova, and J. Byrnes, "A new complementary waveform technique for radar signals", *Proceedings of the IEEE Radar Conference 2002*, 22-25 April 2002, pp. 35-40.

[36] V. C. Vannicola, T. B. Hale, M. C. Wicks, and P. Antonik, "Ambiguity function analysis for the chirp diverse waveform", *Proceedings of the IEEE Radar Conference 2000*, 8-12 May, pp. 666-671.

[37] D. J. Rabideau, "Nonlinear synthetic wideband waveforms", *Proceedings of the IEEE Radar Conference*, Los Angeles, May 2002, pp. 212-219.

[38] E. Mozeson, and N. Levanon, "Removing autocorrelation sidelobes by overlaying orthogonal coding on any train of identical pulses", *IEEE Trans. on Aerospace and Electronic Systems*, Vol. 39, No. 2, pp. 583-603, April 2003.